EuFe2(As1−xPx)2: reentrant spin glass and superconductivity

S. Zapf, H. S. Jeevan, T. Ivek, F. Pfister, F. Klingert, S. Jiang, D. Wu, Philipp Gegenwart, R. K. Kremer, M. Dressel

EuFe$_2$(As$_{1-x}$P$_x$)$_2$: Reentrant Spin Glass and Superconductivity

S. Zapf,[1] H. S. Jeevan,[2] T. Ivek,[1,*] F. Pfister,[1] F. Klingert,[1] S. Jiang,[1] D. Wu,[1] P. Gegenwart,[2]
R. K. Kremer,[3] and M. Dressel[1]

[1]*1. Physikalisches Institut, Universität Stuttgart, Pfaffenwaldring 57, 70550 Stuttgart, Germany*
[2]*I. Physikalisches Institut, Georg-August Universität Göttingen, Friedrich-Hund-Platz 1, 37077 Göttingen, Germany*
[3]*Max-Planck-Institut für Festkörperforschung, Heisenbergstrasse 1, 70569 Stuttgart, Germany*

By systematic investigations of the magnetic, transport, and thermodynamic properties of single crystals of EuFe$_2$(As$_{1-x}$P$_x$)$_2$ ($0 \leq x \leq 1$), we explore the complex interplay of superconductivity and Eu^{2+} magnetism. Below 30 K, two magnetic transitions are observed for all P substituted crystals, suggesting a revision of the phase diagram. In addition to the canted A-type antiferromagnetic order of Eu^{2+} at ~20 K, a spin glass transition is discovered at lower temperatures. Most remarkably, the reentrant spin glass state of EuFe$_2$(As$_{1-x}$P$_x$)$_2$ coexists with superconductivity around $x \approx 0.2$.

The interplay of magnetism and superconductivity is one of the central topics in contemporary condensed matter research. On one hand, their antagonism has been known for a century; on the other hand, superconductivity was found to be closely linked to magnetism, for example, in strongly correlated heavy fermion compounds or high-T_c cuprates as well as in the recently found iron-based pnictide or chalcogenide superconductors [1–4]. In the latter families, systems containing magnetic rare earth elements such as the pnictide superconductor parent compounds CeFeAsO as well as EuFe$_2$As$_2$ are of particular interest, as (besides the spin density wave in the FeAs layers) they develop an additional magnetic order of local moments at low temperatures [5–9]. In the case of CeFeAsO, Ce^{3+} antiferromagnetism appears at ~4 K, whereas EuFe$_2$As$_2$ orders at ~19 K with an A-type antiferromagnetic structure with the Eu^{2+} moments being aligned ferromagnetically along the a axis and antiferromagnetically along the c axis. EuFe$_2$As$_2$ variants are especially fascinating since, despite the proximity of the magnetic and the superconductivity phases observed at rather high temperatures, there is little variation of their transition temperatures T_m and $T_{c,\max}$, respectively. For instance, electron doped Eu(Fe$_{1-x}$Co$_x$)$_2$As$_2$ [10], hole doped K$_x$Eu$_{1-x}$Fe$_2$As$_2$ [11], chemically pressurized EuFe$_2$(As$_{1-x}$P$_x$)$_2$ [12–14], or Eu(Fe$_{1-x}$Ru$_x$)$_2$As$_2$ [15], as well as EuFe$_2$As$_2$ under hydrostatic pressure [16,17], were found to exhibit superconductivity with $T_{c,\max}$ between 20 and 30 K and simultaneously magnetic order with T_m between 10 and 20 K. However, up to now, there is neither a clear picture of how superconductivity can coexist with the strong Eu^{2+} magnetism nor a consensus on the magnetic order in the superconducting phase.

Here, we report our systematic study of the superconducting and magnetic properties of a complete set of EuFe$_2$(As$_{1-x}$P$_x$)$_2$ ($x = 0$, 0.055, 0.09, 0.12, 0.16, 0.165, 0.17, 0.26, 0.35, 0.39, 1) single crystals using dc and ac

magnetization, dc resistivity, and heat capacity measurements. Crystals were prepared and analyzed according to standard procedures [18]. Magnetization data are taken in different modes: either during cooling in an applied field [field cooled cooling (FCC)] or while warming up after the specimen has been cooled in zero field [zero field cooling (ZFC)] or with a magnetic field applied [field cooled heating (FCH)]. For all P substituted specimens, we detect two consecutive magnetic transitions separated by 1.5 K ≲ $\Delta T \lesssim$ 10 K, requiring a revision of the phase diagram of EuFe$_2$(As$_{1-x}$P$_x$)$_2$. Magnetic ordering at a higher temperature is associated with predominant antiferromagnetic interlayer coupling, probably canted A-type antiferromagnetism, whereas the second transition at lower temperatures is identified as a spin glasslike transition evidenced by characteristic frequency dependence and thermal hysteresis effects. We conclude that the development of superconductivity is supported by the decoupling of the magnetic Eu^{2+} layers in the glass phase, which could be the key to understanding the interplay of superconductivity and rare earth magnetism.

EuFe$_2$P$_2$.—The magnetic properties of polycrystalline EuFe$_2$P$_2$ samples have been already investigated by Mössbauer, specific heat and magnetization measurements [19], and neutron powder diffraction [20]. Whereas Ryan *et al.* interpreted their neutron diffraction data in terms of a single phase ferromagnetic transition at ~30 K, Feng *et al.* reported a broad smeared heat capacity anomaly. In analogy to the magnetic behavior of Eu(Fe$_{0.89}$Co$_{0.11}$)$_2$As$_2$ [10], they tentatively analyzed their data in terms of a ferromagnetic and a subsequent "possible helimagnetic ordering."

Figure 1 shows the in-plane ($H\|ab$) magnetic behavior of our EuFe$_2$P$_2$ single crystal [21]. In a very small probing field of 2 G, two consecutive magnetic transitions can be clearly resolved in the ZFC and FCC dc magnetic susceptibility. A sharp peak at $T_1 \approx 29$ K is followed by an upturn starting at $T_2 \approx 27.7$ K, leading to a second peak
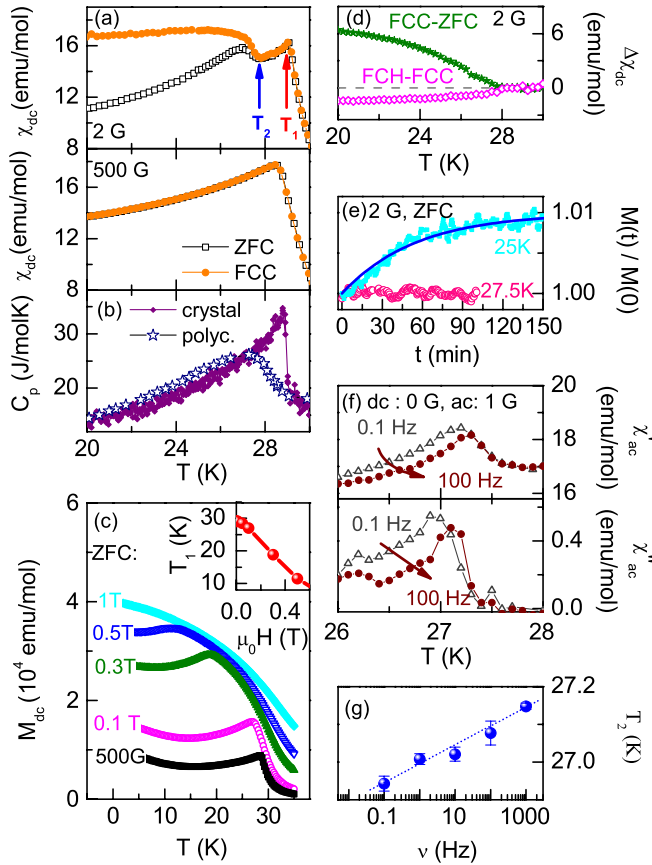
FIG. 1 (color online). $H\|ab$ magnetization of $EuFe_2P_2$.
(a) The ZFC (black open squares) and FCC (orange dots) curves
at 2 G show two consecutive magnetic transitions T_1 and T_2,
with a strong hysteresis at $T < T_2$ (upper panel). The transition
at T_2 is completely suppressed with $\mu_0 H = 500$ G (lower
panel). (b) The heat capacity for our single crystal (purple filled
diamonds) and for polycrystalline $EuFe_2P_2$ [24] (open dark blue
stars) shows a broad feature covering the two magnetic transi-
tions. (c) ZFC magnetization for 500 G, 0.1 T, 0.3 T, 0.5 T, and
1 T. T_1 decreases with increasing external field, also depicted in
the inset. (d) Magnetic hysteresis sets in at $T < T_2$, visible in
$\chi_{dc,FCC} - \chi_{dc,ZFC} > 0$ (filled green stars) ($\mu_0 H = 2$ G). Time
dependence for $T < T_2$ is revealed by FC cycling, visible in
$\chi_{dc,FCH} - \chi_{dc,FCC} < 0$ (open pink diamonds) and (e) time-
dependent magnetization after ZFC cooling ($\mu_0 H = 2$ G;
open pink circles, 27.5 K; closed blue squares, 25 K; dark blue
line, fit of 25 K data). (f) Frequency dependence in ac suscep-
tibility $\chi'_{ac}(T)$ and $\chi''_{ac}(T)$ (no dc field; ac drive amplitude 1 G;
0.1 Hz, dark grey open triangles; 100 Hz, filled brown dots) also
sets in below T_2. (g) Vogel-Fulcher fit of the peak below T_2
in $\chi''_{ac}(T)$.

at ~27 K in the ZFC magnetization [see Fig. 1(a)].
Whereas the transition at T_1 exhibits no thermal hysteresis,
the second transition at T_2 is characterized by a pro-
nounced ZFC-FCC hysteresis which vanishes if a larger
dc magnetic field ($H\|ab$) is applied. It can be finally sup-
pressed for fields above 500 G. Increasing the field even
higher shifts the peak at T_1 down [see Fig. 1(c)], and at
around 1 T, the peak has completely disappeared. Note that

a broad shoulder develops at ~0.3 T, which for $EuFe_2As_2$
was interpreted as due to a metamagnetic transition [6].
Specific heat measurements on the single crystal show a
sharp peak at T_1 with a broad shoulder at lower tempera-
tures, consistent with the width of the anomaly for poly-
crystalline samples reported in Ref. [19], and prove that
both transitions are bulk properties. In order to get more
insight into the character of the second transition at T_2, we
studied in detail its thermal hysteresis and frequency de-
pendence by ac magnetization measurements. Figure 1(d)
displays the differences between the ZFC, FCC, and FCH
susceptibilities for an in-plane field of 2 G. The thermal
hysteresis is visible in the ZFC-FCC splitting at $T < T_2$.
Repeated FCC and FCH cycles (heating or cooling rates
0.2 K/min) revealed a very slow time dependence of the
magnetization below T_2, leading to a growth of the magne-
tization and consequently a negative difference of FCH −
FCC. The time dependence of the magnetization below T_2
is also visible in the time dependence of the ZFC magne-
tization, which after some rapid initial increase grows
exponentially [see Fig. 1(e)] with a relaxation time of
~2200 s, in good agreement with other (reentrant) spin
glass systems [23]. The time dependence of the magneti-
zation also becomes apparent in the frequency-dependent
real and imaginary components of the ac susceptibility χ'_{ac}
and χ''_{ac}, as depicted in Fig. 1(f). Below T_2, a peak appears in
both components ($\chi'_{ac} \approx 50 \times \chi''_{ac}$), which shifts to a higher
temperature with increasing frequency following a Vogel-
Fulcher behavior [see Fig. 1(g)]. We can rule out any relation
of the time and frequency dependence to flux line lattice
dynamics since $EuFe_2P_2$ is far off from any proposed super-
conducting phase [12,13].

Until now, magnetic ordering at higher P concen-
trations in polycrystalline and single crystalline samples
of $EuFe_2(As_{1-x}P_x)_2$ was assigned to ferromagnetism
[12,13,24]. Spin canting with a ferromagnetic net
component along the c axis has been concluded from
Mössbauer and magnetization measurements on mixed
$EuFe_2(As_{1-x}P_x)_2$ samples [22,24]. Measurements on
polycrystalline samples [13,24], however, are not able to
allow conclusions about possible antiferromagnetic inter-
layer coupling, and measurements on single crystals of
$EuFe_2(As_{1-x}P_x)_2$ [12] failed to reveal two separate mag-
netic transitions and their different thermal hysteretic
behavior because of too coarse temperature steps. In view
of the shape of the $M(T)$ anomaly at T_1 [see Fig. 1(b)], we
suggest that the Eu^{2+} moments in $EuFe_2P_2$ order rather with
a canted A-type antiferromagnetic structure [25] with the
spin components being ferromagnetically aligned along the c
axis. Additionally, below T_2, we detect a second phase
transition with glassy character which we associate to
the ordering of the in-plane components of the Eu^{2+}
moments. The development of a glassy phase below a
magnetic phase transition, commonly referred to as reentrant
spin glass [23,26–30], indicates a competition between

antiferromagnetic and ferromagnetic spin exchange interactions in the system. In the case of $EuFe_2P_2$, the antiferromagnetic Ruderman-Kittel-Kasuya-Yosida (RKKY) interlayer coupling competes with the ferromagnetic intralayer interactions of the spins. In fact, density functional theory-based calculations revealed a very small energy difference of antiferromagnetic and ferromagnetic ground states for $EuFe_2(As_{1-x}P_x)_2$ [12]. We therefore suggest that, in $EuFe_2P_2$, competition between ferro- and antiferromagnetism causes glassy freezing of spin components in the ab plane at T_2 and a decoupling of the magnetic Eu layers. Such a freezing of transverse magnetic compounds following long range magnetic order which has set in is consistent with mean field theoretical calculations for a reentrant spin glass [31]. Our conclusions are not only supported by the time-dependent magnetization behavior at $T < T_2$ but also by the development of $M(T)$ with external fields: by application of a magnetic field of ~ 500 G along the ab plane, the energy barrier between different equilibrium states can be overcome, the glass transition is suppressed, and the temperature-dependent magnetization resembles that of $EuFe_2As_2$. This interpretation is consistent with the neutron powder diffraction studies by Ryan *et al.* [20], as those are not sensitive to the freezing of the small in-plane spin component, as long as the ferromagnetic spin component along the c axis still exists.

$EuFe_2(As_{0.835}P_{0.165})_2$.—In order to study the complex interplay of magnetism and superconductivity in mixed As-P samples, we have investigated in detail the magnetic and superconducting properties of a single crystal of $EuFe_2(As_{0.835}P_{0.165})_2$. The in-plane electrical resistivity [see Fig. 2(a)] proves the onset of superconductivity at $T_{c,on}^* \approx 22$ K indicated by a steep initial decrease of the resistivity. Zooming into the transition reveals reentrant behavior at about 19 K followed by a smooth decrease towards zero resistivity which is achieved only below $T_{\rho=0}^* \approx 9$ K [see Fig. 2(b)]. Figures 2(c)–2(f) compile selected ac and dc magnetization data obtained with experimental configurations identical to those used for $EuFe_2P_2$. The dc magnetizations at low fields, similar to those of $EuFe_2P_2$, show two peaks for $H\|ab$ which are shifted to lower temperatures [$T_1 \approx 19$ K, $T_2 \approx 16.8$ K; see Fig. 2(c)]. A steep downturn occurs below 15 K for both $H\|c$ and $H\|ab$ magnetizations, which ends up in a diamagnetic signal for $H\|c$, indicating superconducting shielding [see Fig. 2(d)]. As $H\|ab$ requires shielding currents perpendicular to the layers, the magnetization stays positive. However, performing in-plane ac susceptibility measurements with applied high dc fields $H\|ab$ [see Fig. 2(e)] also reveals a diamagnetic in-plane shielding signal if the dc field is large enough ($\gtrsim 1$ T) to saturate the Eu^{2+} magnetism.

Repeated field cooled (FC) cycling again reveals a time dependence of the magnetization with a negative FCH − FCC difference below $T < T_2$ characteristic of
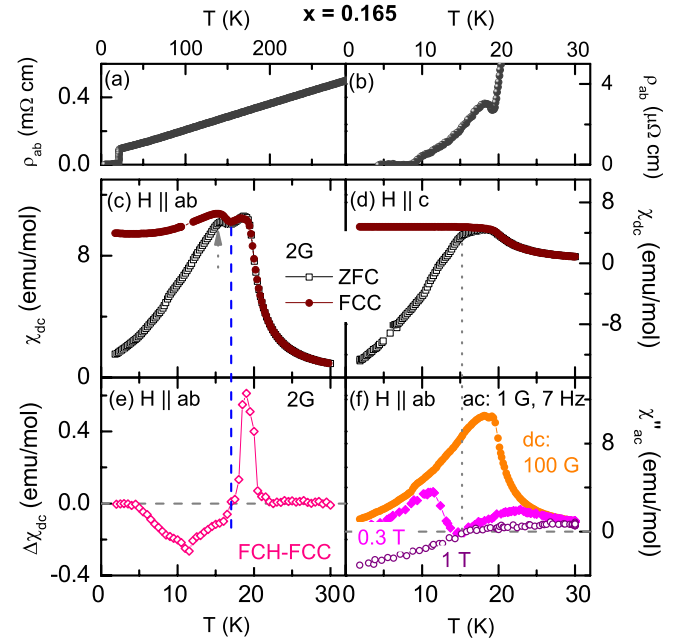

FIG. 2 (color online). $EuFe_2(As_{0.835}P_{0.165})_2$. In-plane resistivity $\rho_{ab}(T)$ shows (a) linear temperature dependence at high temperature and (b) reentrant superconductivity with onset $T_{c,on}^* \approx 22$ K and zero resistivity $T_{\rho=0}^* \approx 9$ K. ZFC (black open squares) as well as FCC (filled brown dots) magnetization shows for (c) $H\|ab$ (2 G) two magnetic transitions similar to $x = 1.0$ (T_2 is indicated by a dashed blue line), with a steep drop in the ZFC curve below ~ 15 K (dotted grey arrow), which also appears for (d) $H\|c$ (dotted grey line), where negative magnetization is reached. (e) FC cycling reveals two time-dependent glassy transitions, as FCH − FCC > at $T < T_{c,on}$ and FCH − FCC < at $T < T_2$. (f) Combining ac susceptibility measurements (drive 1 G, frequency 7 Hz) with high dc fields (100 G, filled orange dots; 0.3 T, filled pink diamonds; 1 T, open purple circles), negative magnetization is revealed for $H\|ab$ below 15 K (dotted grey line).

glassy magnetism, similar to that found in $EuFe_2P_2$ [see Fig. 1(c)]. We therefore conclude that superconducting $EuFe_2(As_{0.835}P_{0.165})_2$ shows an analogous reentrant spin glass behavior as $EuFe_2P_2$. The additional positive peak in the FCH − FCC curve between 17 and 21 K could be ascribed to vortex dynamics, as it coincides with the steep initial decrease of the resistivity marking the onset of superconductivity.

Phase diagram.—In order to follow compositional dependence of the two magnetic transitions consistently found in $EuFe_2P_2$ and $EuFe_2(As_{0.835}P_{0.165})_2$, we have extended our studies to $EuFe_2(As_{1-x}P_x)_2$ single crystals with $x = 0$, 0.055, 0.09, 0.12, 0.16, 0.17, 0.26, 0.35, and 0.39 (see Fig. 3). In all P substituted specimens, we observe two consecutive magnetic transitions, which we ascribe, in analogy to the previous sections, to a canted A-type antiferromagnetic (AFM) transition with the Eu^{2+} spin components along the c axis being ferromagnetically aligned below $T_1 = T_{cAFM}$ and to a glassy freezing of the spin components in
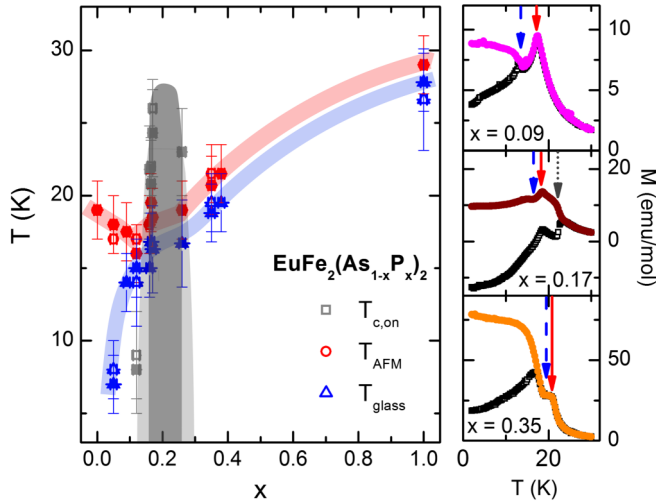
FIG. 3 (color online). Phase diagram of $EuFe_2(As_{1-x}P_x)_2$. T_{cAFM} (red dots) indicates a canted A-type antiferromagnetic transition, with a ferromagnetic net component of the Eu^{2+} spins along the c direction, T_{glass} (blue triangles) a spin glass transition due to the freezing of the spins in the ab plane, and $T_{c,on}$ the onset of superconductivity (grey squares). Closed symbols indicate transition temperatures deduced from magnetization, open ones temperatures deduced from resistivity measurements. Shadowed lines are guides to the eye. The light grey area indicates the onset of superconductivity, while bulk superconductivity is fully developed in the dark grey regime [12,36]. The right panel shows typical corresponding $M(T)$ curves. Nonsuperconducting $x = 0.09$ (ZFC, open squares; FCC, pink dots), superconducting $x = 0.17$ (ZFC, open squares; FCC, brown dots), as well as nonsuperconducting $x = 0.35$ (ZFC, open squares; FCC, orange dots) samples are selected. Arrows indicate the transition temperatures for the antiferromagnetic (solid red lines), spin glass (dashed blue lines), and superconducting (dotted grey line) phases.

the ab plane at $T_2 = T_{glass}$, with $T_{cAFM} > T_{glass}$. In Fig. 3, we have compiled the resulting magnetic phase diagram together with the superconducting dome.

According to our investigations on single crystals, the reentrant spin glass transition appears for all P substituted specimens. The effect of chemical disorder of the As and P anions on the RKKY exchange must be ruled out as the origin of the glass transition since it also occurs in well-ordered $EuFe_2P_2$ crystals. We rather ascribe the glass transition to competition of ferromagnetic interactions within a layer with antiferromagnetic RKKY interactions between neighboring layers.

The transition temperatures exhibit a nonmonotonic behavior with P substitution. At low P concentration $0 < x \lesssim 0.12$, the antiferromagnetic Eu^{2+} transition temperature follows the transition temperature of the spin density wave. Coupling of the itinerant Fe magnetism and the Eu^{2+} local spin moments was theoretically predicted and experimentally confirmed by the increasing canting of spins out of the ab plane concomitant with the suppression of the spin density wave [22,24,32,33]. With

increasing canting, the ferromagnetic component of the Eu^{2+} along the c direction increases, and the competition with the antiferromagnetic RKKY interaction between the layers is enhanced, which finally leads to the development of the spin glass phase. In the superconducting regime, the transition temperatures vary only slightly with P concentration. When superconductivity is finally suppressed, both transition temperatures T_1 and T_2 increase markedly, probably due to a Lifshitz transition [34–36] which effects the RKKY exchange.

Antiferromagnetic interlayer coupling developing up to high P concentrations, as well as a rather narrow superconducting dome, are consistent with experiments on $EuFe_2As_2$ under pressure [17]. Between the concentrations $x \approx 0.12$ and $x \approx 0.26$, the onset of a superconducting transition is found, while fully developed bulk superconductivity occurs in an even narrower regime [12,36]. As concluded previously, a Lifshitz transition near $x \approx 0.23$ coincides with the upper limit of superconductivity [34–36]. Investigations of polycrystalline samples, however, resulted in a somewhat broader dome extending to an upper limit of $x \approx 0.4$ [13,24]. The assignment of the upper limit was based on the assumption that two subsequent resistivity anomalies seen in samples with $x \approx 0.4$ indicate the onset of superconductivity succeeded by reentrance due to ordering of the Eu^{2+} spins. Our experiments on single crystals rather indicate that these two anomalies are purely of magnetic origin, as we do not see any signature of superconductivity in our $x = 0.35$ crystal (see Fig. 3, right panel) [37].

The question of how bulk superconductivity can coexist with Eu^{2+} magnetic ordering is quite fundamental and requires the exact knowledge of the magnetic structure. Consistent with Mössbauer and neutron powder diffraction [20,24], the results of our experiments imply that a large net component of the Eu^{2+} spins is ferromagnetically aligned perpendicular to the layers. In addition, we find that glass-like dynamics and freezing of the in-plane component develops below T_2, which destroys coherence between the Eu layers. Superconductivity in the iron-based superconductors is commonly believed to take place mainly in the FeAs layers. In this scenario, the inner field resulting from the Eu^{2+} ferromagnetic component along the c axis could be screened by the formation of spontaneous vortices perpendicular to the layers [15]. Together with the destroyed coherence between the Eu layers due to the glass dynamics, this scenario might be key to how superconductivity can coexist with the usually strong Eu^{2+} magnetism. It will be therefore very interesting to also investigate other Eu containing pnictides in more detail in order to understand whether the glass phase is required for the existence of superconductivity in these systems.

Conclusion.—$EuFe_2(As_{1-x}P_x)_2$ exhibits two consecutive magnetic transitions $T_{cAFM} > T_{glass}$ over the entire P substitution range. From magnetization data, we identify

the higher temperature transition as a canted A-type antiferromagnetic transition. The spin canting increases with P substitution concomitant with the suppression of the spin density wave, until the spins are aligned almost along the c direction; i.e., ferromagnetic intralayer coupling competes with antiferromagnetic RKKY interlayer coupling. This causes glassy behavior of the spin components in the ab plane at T_{glass}, evidenced by the characteristic frequency- and time-dependent response of the magnetization. Thus, $EuFe_2(As_{1-x}P_x)_2$ is a reentrant spin glass and does not sustain conventional antiferromagnetic or ferromagnetic Eu^{2+} magnetic ordering down to low temperatures. Development of superconductivity is supported by the decoupling of the magnetic Eu^{2+} layers.

———

*Also at Institut za fiziku, Post Office Box 304, HR-10001 Zagreb, Croatia.

[1] D. C. Johnston, Adv. Phys. **59**, 803 (2010).

[2] I. I. Mazin, Nature (London) **464**, 183 (2010).

[3] M. R. Norman, Science **332**, 196 (2011).

[4] I. I. Mazin, Physics **4**, 26 (2011).

[5] J. Zhao, Q. Huang, C. Cruz, S. Li, J. W. Lynn, Y. Chen, M. A. Green, G. F. Chen, G. Li, Z. Li, J. L. Luo, N. L. Wang, and P. Dai, Nat. Mater. **7**, 953 (2008).

[6] S. Jiang, Y. Luo, Z. Ren, Z. Zhu, C. Wang, X. Xu, Q. Tao, G. Cao, and Z. Xu, New J. Phys. **11**, 025007 (2009).

[7] Y. Xiao, Y. Su, M. Meven, R. Mittal, C. M. N. Kumar, T. Chatterji, S. Price, J. Persson, N. Kumar, S. K. Dhar, A. Thamizhavel, and Th. Brueckel, Phys. Rev. B **80**, 174424 (2009).

[8] Y. Xiao, Y. Su, W. Schmidt, K. Schmalzl, C. M. N. Kumar, S. Price, T. Chatterji, R. Mittal, L. J. Chang, S. Nandi, N. Kumar, S. K. Dhar, A. Thamizhavel, and T. Brueckel, Phys. Rev. B **81**, 220406(R) (2010).

[9] M. Tegel, M. Rotter, V. Weiß, F. M. Schappacher, R. Pöttgen, and D. Johrendt, J. Phys. Condens. Matter **20**, 452201 (2008).

[10] S. Jiang, H. Xing, G. Xuan, Z. Ren, C. Wang, Z. A. Xu, and G. Cao, Phys. Rev. B **80**, 184514 (2009).

[11] H. S. Jeevan, Z. Hossain, D. Kasinathan, H. Rosner, C. Geibel, and P. Gegenwart, Phys. Rev. B **78**, 092406 (2008).

[12] H. S. Jeevan, D. Kasinathan, H. Rosner, and P. Gegenwart, Phys. Rev. B **83**, 054511 (2011).

[13] G. Cao, S. Xu, Z. Ren, S. Jiang, C. Feng, and Z. A. Xu, J. Phys. Condens. Matter **23**, 464204 (2011).

[14] Z. Ren, Q. Tao, S. Jiang, C. Feng, C. Wang, J. Dai, G. Cao, and Z. Xu, Phys. Rev. Lett. **102**, 137002 (2009).

[15] W. H. Jiao, Q. Tao, J. K. Bao, Y. L. Sun, C. M. Feng, Z. A. Xu, I. Nowik, I. Felner, and G. H. Cao, Europhys. Lett. **95**, 67007 (2011).

[16] T. Terashima, M. Kimata, H. Satsukawa, A. Harada, K. Hazama, S. Uji, H. S. Suzuki, T. Matsumoto, and K. Murata, J. Phys. Soc. Jpn. **78**, 083701 (2009).

[17] K. Matsubayashi, K. Munakata, M. Isobe, N. Katayama, K. Ohgushi, Y. Ueda, Y. Uwatoko, N. Kawamura, M. Mizumaki, N. Ishimatsu, M. Hedo, and I. Umehara, Phys. Rev. B **84**, 024502 (2011).

[18] See Supplemental Material at http://link.aps.org/supplemental/10.1103/PhysRevLett.110.237002 for more details of the crystal preparation (cf. Ref. [12]) and experimental techniques.

[19] C. Feng, Z. Ren, S. Xu, S. Jiang, Z. A. Xu, G. Cao, I. Nowik, I. Felner, K. Matsubayashi, and Y. Uwatoko, Phys. Rev. B **82**, 094426 (2010).

[20] D. H. Ryan, J. M. Cadogan, S. Xu, Z. A. Xu, and G. Cao, Phys. Rev. B **83**, 132403 (2011).

[21] The out-of-plane magnetization $M(T)$ is almost flat below T_1, with a small splitting due to a ferromagnetic net component along the c axis (similar to $x = 0.35$; see Ref. [22]). Supplemental information will be available on request.

[22] S. Zapf, D. Wu, L. Bogani, H. S. Jeevan, P. Gegenwart, and M. Dressel, Phys. Rev. B **84**, 140503(R) (2011).

[23] B. Maji, K. G. Suresh, and A. K. Nigam, J. Phys. Condens. Matter **23**, 506002 (2011).

[24] I. Nowik, I. Felner, Z. Ren, G. H. Cao, and Z. A. Xu, J. Phys. Condens. Matter **23**, 065701 (2011).

[25] Because of sample shape effects, we cannot distinguish between A-type antiferromagnetism and helimagnetism.

[26] T. Datta, D. Thornberry, E. R. Jones, Jr., and H. M. Ledbetter, Solid State Commun. **52**, 515 (1984).

[27] I. A. Campbell, S. Senoussi, F. Varret, J. Teillet, and A. Hamzić, Phys. Rev. Lett. **50**, 1615 (1983).

[28] A. C. D. van Enter and J. L. van Hemmen, Phys. Rev. B **31**, 603 (1985).

[29] K. Jonason, J. Mattsson, and P. Nordblad, Phys. Rev. B **53**, 6507 (1996).

[30] J. A. Mydosh, *Spin Glasses: An Experimental Introduction* (Taylor & Francis, London, 1993).

[31] M. Gabay and G. Toulouse, Phys. Rev. Lett. **47**, 201 (1981).

[32] A. Akbari, I. Eremin, and P. Thalmeier, Phys. Rev. B **84**, 134513 (2011).

[33] A. Akbari, P. Thalmeier, and I. Eremin, New J. Phys. **15**, 033034 (2013).

[34] J. Maiwald, H. S. Jeevan, and P. Gegenwart, Phys. Rev. B **85**, 024511 (2012).

[35] S. Thirupathaiah, E. D. L. Rienks, H. S. Jeevan, R. Ovsyannikov, E. Slooten, J. Kaas, E. van Heumen, S. de Jong, H. A. Durr, K. Siemensmeyer, R. Follath, P. Gegenwart, M. S. Golden, and J. Fink, Phys. Rev. B **84**, 014531 (2011).

[36] Y. Tokiwa, S. H. Hübner, O. Beck, H. S. Jeevan, and P. Gegenwart, Phys. Rev. B **86**, 220505(R) (2012).

[37] The double feature in $M(T)$ curves for superconducting samples was in some cases assigned to result from the paramagnetic Meissner effect [24]. However, this effect should only appear in the FC curve [38], whereas features are also observed in ZFC data.

[38] W. Braunisch, N. Knauf, V. Kataev, S. Neuhausen, A. Grütz, A. Kock, B. Roden, D. Khomskii, and D. Wohlleben, Phys. Rev. Lett. **68**, 1908 (1992).